Geometrically Nonlinear Transient Analysis of Laminated Composite Plates

J. N. Reddy*
Virginia Polytechnic Institute and State University, Blacksburg, Virginia

Forced motions of laminated composite plates are investigated using a finite element that accounts for the transverse shear strains, rotary inertia, and large rotations (in the von Kármán sense). The present results when specialized for isotropic plates are found to be in good agreement with those available in the literature. Numerical results of the nonlinear analysis of composite plates are presented showing the effects of plate thickness, lamination scheme, boundary conditions, and loading on the deflections and stresses. The new results for composite plates should serve as bench marks for future investigations.

Nomenclature

A_{ij},B_{ij},D_{ij}	= extensional, flexural extensional, and flexural stiffnesses $(i,j=1,2,6)$
a,b	= plate planform dimensions of x,y directions
a_0,a_1,etc.	= parameters in the time approximation, see Eq. (15)
E_1,E_2	= layer elastic moduli in directions along fibers and normal to them, respectively
G_{12},G_{13},G_{23}	= layer inplane and thickness shear moduli
h	= total thickness of the plate
I	= rotatory inertia coefficient per unit midplane area of layer
k_i	= shear correction coefficient associated with the yz and xz planes, respectively $(i=4,5)$
M_i,N_i	= stress couple and stress resultant, respectively $(i=1,2,6)$
P	= laminate normal inertia coefficient per unit midplane area
Q_i	= shear stress resultant $(i=1,2)$
Q_{ij}	= plane-stress reduced stiffness coefficients $(i,j=1,2,6)$
R	= laminate rotatory-normal coupling inertia coefficient per unit midplane area
u,v,w	= displacement components in x,y,z directions, respectively
U_i,V_i,W_i	= nodal values of displacements u,v,w $(i=1,2,...,n)$
x,y,z	= position coordinates in Cartesian system
$\{\Delta\}$	= column vector of generalized nodal displacements
α,β	= parameters in the Newmark integration scheme
ϵ_i	= strain components $(i=1,2,...,6)$
θ_m	= orientation of mth layer $(m=1,2,...,L)$
$\rho^{(m)}$	= density of mth layer $(m=1,2,...,L)$
σ_i	= stress components $(i=1,2,...,6)$
ϕ_i	= finite element interpolation functions $(i=1,2,...,n)$
ψ_x,ψ_y	= bending slope (rotation) functions

Introduction

THE transient behavior of isotropic and homogeneous plates has long been a subject of interest (see Lamb[1] for thin plates and David and Lawhead[2] for thick plates). For many years, the classical (Poisson-Kirchoff) plate theory (CPT), in which normals to the midsurface before deformation are assumed to remain straight and normal to the midsurface after deformation (i.e., transverse shear strains are zero), has been used to calculate frequencies, static response, and dynamic response under applied loads. Recent studies in the analysis of plates have shown that the effect of the transverse shear strains on the static and dynamic response of plates is significant. For example, the natural frequencies of vibration predicted by the classical plate theory are 25% higher, for plate side-to-thickness ratio of 10, than those predicted by a shear deformation theory (SDT). In transient analysis of plates the classical plate theory predicts unrealistically large phase velocities in the plate for shorter wavelengths. The Timoshenko beam theory,[3] which includes transverse shear and rotary inertia effects, has been extended to isotropic plates by Reissner[4,5] and Mindlin,[6] and to laminated anisotropic plates by Yang et al.[7] A generalization of the von Kármán nonlinear plate theory for isotropic plates to include the effects of transverse shear and rotary inertia in the theory of orthotropic plates is due to Medwadawski,[8] and that for anisotropic plates is due to Ebcioglu.[9]

With the increased application of advanced fiber composite material to jet engine fan or compressor blades, and in high performance aircraft, studies involving transient response of plates made of such materials are needed to assess the capability of these materials to withstand the forces of impact due to foreign objects (e.g., the ingestion of stones, nuts and bolts, hailstones, or birds in jet engines). Previous investigations into the linear transient analysis of composite plates include Moon's[10,11] investigation of the response of infinite laminated plates subjected to transverse impact loads at the center of the plate; Chow's[12] study of laminated plates (with transverse shear and rotary inertia) using the Laplace transform technique; the Wang et al.[13] investigation, by the method of characteristics, of unsymmetrical orthotropic laminated plates; and Sun and Whitney's[14,15] study of plates under cylindrical bending. More recently, the present author[16,17] investigated the linear transient response of layered anisotropic composite rectangular plates and presented extensive numerical results for center deflection and stresses.

Geometrically nonlinear transient analysis of isotropic plates was considered by Hinton et al.[18-20] and Akay.[21] Hinton et al. used the Mindlin element while Akay used a mixed finite element in their works. As far as the nonlinear (geometric) analysis of layered anisotropic composite plates is concerned, there exist no previously reported results in the open literature. The present investigation is concerned with the geometrically nonlinear transient analysis of layered composite plates under applied transverse loads. The shear deformable element developed by the author[17] for the transient analysis of layered composite plates is modified to include the nonlinear strain-displacement relations of the von

Received April 2, 1982; revision received July 22, 1982.

*Professor, Department of Engineering Science and Mechanics.

Kármán plate theory. Numerical results are presented to show the effect of lamination scheme, plate thickness, nonlinearity, boundary conditions, and loading on the transient response of plates. The numerical results included here for layered composite plates are not available in the literature, and, therefore, should be of interest to designers of composite-plate structures and numerical analysts and experimentalists in evaluating their techniques.

Review of the Equations of Motion of Anisotropic Plates

The nonlinear theory of laminated anisotropic plates to be reviewed is based on the combination of the Timoshenko-type theory and the von Kármán plate theory. The theory is known to be able to predict accurately the global behavior. However, it is not accurate enough to predict edge stresses and, hence, delamination. The theory assumes that the stresses normal to the midplane of the plate are negligible when compared to the inplane stresses, and normals to the plate midsurface before deformation remain straight but not necessarily normal to the midsurface after deformation.

Equations of Motion

The plate under consideration is composed of a finite number of orthotropic layers of uniform thickness, with principal axes of elasticity oriented arbitrarily with respect to the plate axes. The x and y coordinates of the plate are taken in the midplane (Ω) of the plate. As in all Timoshenko-type theories, the displacement field is assumed to be of the form

$$u_1(x,y,z,t)=u(x,y,t)+z\psi_x(x,y,t)$$

$$u_2(x,y,z,t)=v(x,y,t)+z\psi_y(x,y,t)$$

$$u_3(x,y,z,t)=w(x,y,t) \tag{1}$$

Here t is the time; u_1, u_2, u_3 the displacements in the x, y, z directions, respectively; u, v, w the associated midplane displacements; and ψ_x and ψ_y the slopes in the xz and yz planes due to bending only. The strains in the von Kármán plate theory (which accounts for moderately large deflections and small strains) can be expressed in the form

$$\epsilon_1=\frac{\partial u}{\partial x}+\frac{1}{2}\left(\frac{\partial w}{\partial x}\right)^2+z\frac{\partial\psi_x}{\partial x}\equiv\epsilon_1^0+z\kappa_1$$

$$\epsilon_2=\frac{\partial v}{\partial y}+\frac{1}{2}\left(\frac{\partial w}{\partial y}\right)^2+z\frac{\partial\psi_y}{\partial y}\equiv\epsilon_2^0+z\kappa_2$$

$$\epsilon_6=\frac{\partial u}{\partial y}+\frac{\partial v}{\partial x}+\frac{\partial w}{\partial x}\frac{\partial w}{\partial y}+z\left(\frac{\partial\psi_x}{\partial y}+\frac{\partial\psi_y}{\partial x}\right)\equiv\epsilon_6^0+z\kappa_6$$

$$\epsilon_5=\psi_x+\frac{\partial w}{\partial x},\quad \epsilon_4=\psi_y+\frac{\partial w}{\partial y} \tag{2}$$

wherein the squares of the first spatial derivatives of u, v, ψ_x, and ψ_y are neglected. The strain ϵ_3 does not enter the equations because the constitutive relations, to be given shortly, are based on the plane-stress assumption. Note that the transverse shear strains, ϵ_4 and ϵ_5, are constant through the thickness. If a linear distribution of the transverse shear strains through the thickness is desired, one must add higher order terms in z to the displacement u_1 and u_2, and/or u_3; with each additional term, an additional dependent variable is introduced into the problem.

Neglecting the body moments and surface shearing forces, we write the equations of motion in the presence of applied transverse forces q as

$$N_{1,x}+N_{6,y}=Pu_{,tt}+R\psi_{x,tt}$$

$$N_{6,x}+N_{2,y}=Pv_{,tt}+R\psi_{y,tt}$$

$$Q_{1,x}+Q_{2,y}=Pw_{,tt}+q(x,y,t)+\mathfrak{N}(w,N_i)$$

$$M_{1,x}+M_{6,y}-Q_1=I\psi_{x,tt}+Ru_{,tt}$$

$$M_{6,x}+M_{2,y}-Q_2=I\psi_{y,tt}+Rv_{,tt} \tag{3}$$

where P, R, and I are the normal, coupled normal rotary, and rotary inertia coefficients, respectively,

$$(P,R,I)=\int_{-h/2}^{h/2}(1,z,z^2)\rho\,\mathrm{d}z=\sum_m\int_{z_m}^{z_{m+1}}(1,z,z^2)\rho^{(m)}\mathrm{d}z \tag{4}$$

$\rho^{(m)}$ being the material density of the mth layer; N_i, Q_i, and M_i are the stress and moment resultants defined by

$$(N_i,M_i)=\int_{-h/2}^{h/2}(1,z)\sigma_i\mathrm{d}z,\quad (Q_1,Q_2)=\int_{-h/2}^{h/2}(\sigma_5,\sigma_4)\mathrm{d}z \tag{5}$$

and $\mathfrak{N}(w,N_i)$ is the contribution due to the nonlinear terms

$$\mathfrak{N}(w,N_i)=\frac{\partial w}{\partial x}\left(\frac{\partial N_1}{\partial x}+\frac{\partial N_6}{\partial y}\right)+\frac{\partial w}{\partial y}\left(\frac{\partial N_6}{\partial x}+\frac{\partial N_2}{\partial y}\right) \tag{6}$$

Here σ_i ($i=1,2,\ldots,6$) denote the inplane stress components ($\sigma_1=\sigma_x$, $\sigma_2=\sigma_y$, $\sigma_4=\sigma_{zy}$, $\sigma_5=\sigma_{xz}$, and $\sigma_6=\sigma_{xy}$).

If one plane of elastic symmetry parallel to the plane of each layer exists, the constitutive equations for the plate can be written in the form (see Ref. 22)

$$\begin{Bmatrix} N_i \\ M_i \end{Bmatrix}=\begin{bmatrix} A_{ij} & B_{ij} \\ B_{ji} & D_{ij} \end{bmatrix}\begin{Bmatrix} \epsilon_j^0 \\ K_j \end{Bmatrix}$$

$$\begin{Bmatrix} Q_2 \\ Q_1 \end{Bmatrix}=\begin{bmatrix} \bar{A}_{44} & \bar{A}_{45} \\ \bar{A}_{45} & \bar{A}_{55} \end{bmatrix}\begin{Bmatrix} \epsilon_4 \\ \epsilon_5 \end{Bmatrix} \tag{7}$$

The A_{ij}, B_{ij}, D_{ij} ($i,j=1,2,6$), and $\bar{A}_{ij}$ ($i,j=4,5$) are the inplane, bending inplane coupling, bending or twisting, and thickness-shear stiffnesses, respectively:

$$(A_{ij},B_{ij},D_{ij})=\sum_m\int_{z_m}^{z_{m+1}}Q_{ij}^{(m)}(1,z,z^2)\mathrm{d}z$$

$$\bar{A}_{ij}=\sum_m\int_{z_m}^{z_{m+1}}k_ik_jQ_{ij}^{(m)}\mathrm{d}z \tag{8}$$

Here, z_m denotes the distance from the midplane to the lower surface of the mth layer, and k_i are the shear correction coefficients.

Variational Formulation

The variational form of Eqs. (3) and (7) is given by

$$0=\int_\Omega \Big\{\delta u(Pu_{,tt}+R\psi_{x,tt})+\delta u_{,x}N_1+\delta u_{,y}N_6$$
$$+\delta v(Pv_{,tt}+R\psi_{y,tt})+\delta v_{,x}N_6+\delta v_{,y}N_2+\delta w(Pw_{,tt})$$
$$+\delta w_{,x}Q_1+\delta w_{,y}Q_2+\frac{\partial \delta w}{\partial x}\left(\frac{\partial w}{\partial x}N_1+\frac{\partial w}{\partial y}N_6\right)$$
$$+\frac{\partial \delta w}{\partial y}\left(\frac{\partial w}{\partial x}N_6+\frac{\partial w}{\partial y}N_2\right)+\delta\psi_x(I\psi_{x,tt}+Ru_{,tt})+\delta\psi_{x,x}M_1$$
$$+\delta\psi_{x,y}M_6+\delta\psi_xQ_1+\delta\psi_y(I\psi_{y,tt}+Rv_{,tt})+\delta\psi_{y,x}M_6$$
$$+\delta\psi_{y,y}M_2+\delta\psi_yQ_2+\delta wq\Big\}\mathrm{d}x\mathrm{d}y+\int_\Gamma(\delta u_nN_n$$
$$+\delta u_sN_{ns})\mathrm{d}s+\int_\Gamma \delta wV\mathrm{d}s+\int_\Gamma(\delta\psi_nM_n+\delta\psi_sM_{ns})\mathrm{d}s \quad (9)$$

wherein N_i, M_i, and Q_i are given in terms of the generalized displacements by Eq. (7); V, N_n, and N_{ns}, and M_n and M_{ns} are the shear force, normal and tangential inplane forces, and normal and twisting bending moments defined on the boundary Γ, respectively.

$$V=Q_1n_x+Q_2n_y+\left(\frac{\partial w}{\partial x}N_1+\frac{\partial w}{\partial y}N_6\right)n_x$$
$$+\left(\frac{\partial w}{\partial x}N_6+\frac{\partial w}{\partial y}N_2\right)n_y$$
$$N_n=n_xn_xN_1+2n_xn_yN_6+n_yn_yN_2$$
$$N_{ns}=n_xn_y(N_2-N_1)+(n_xn_x-n_yn_y)N_6$$
$$M_n=n_xn_xM_1+2n_xn_yM_6+n_yn_yM_2$$
$$M_{ns}=n_xn_y(M_2-M_1)+(n_xn_x-n_yn_y)M_6 \quad (10)$$

where $\hat{n}=(n_x,n_y)$ is the unit vector normal to the boundary Γ. The variational formulation indicates that the essential (i.e., geometric) and natural boundary conditions of the problem are given by

Essential

specify: $u_n, u_s, w, \psi_n, \psi_s$

Natural

specify: $N_n, N_{ns}, V, M_n, M_{ns}$ (11)

wherein u_n and u_s, for example, denote the normal and tangential components of the inplane displacement vector, $u=(u,v)$.

A Shear-Deformable Finite Element for Laminated Plates

Here we present a finite element model associated with the nonlinear equations governing the motion of layered composite plates. The element is an extension of the penalty plate-bending element developed for the linear static and dynamic analysis of layered composite plates by the present author.[17,23]

Consider a finite element analog Ω_h of the midplane of the plate Ω. Over a typical element, Ω^e of the mesh Ω_h, each generalized displacement U is interpolated spatially by an expression of the form

$$U=\sum_i^r U_i(t)\phi_i(x,y) \quad (12)$$

where U_i is the value of U at node i at time t, ϕ_i is the finite element interpolation function at node i and r is the number of nodes in the element. For the sake of simplicity, we use the same interpolation function for each of the generalized displacements, (u,v,w,ψ_x,ψ_y). Specifically, the nine-node isoparametric rectangular element with five degrees of freedom is used in the present study.

Substituting Eqs. (7) and (12) into Eq. (9), we obtain the following equation

$$[K]\{\Delta\}+[M]\{\ddot{\Delta}\}=\{F\} \quad (13)$$

Here $\{\Delta\}$ is the column vector of the nodal values of the generalized displacements, $[K]$ the matrix of stiffness coefficients, $[M]$ the matrix of mass coefficients, and $\{F\}$ the column vector containing the boundary and transverse force contributions. The elements of $[K]$ and $[M]$ are given in the Appendix.

It should be pointed out that the element stiffness matrix $[K]$ is nonlinear and unsymmetric in the present formulation (see Appendix), the nonlinearity being due to the nonlinear terms appearing in the variational formulation. The nonsymmetric nature of the stiffness matrix needs some explanation. To this end consider the following terms from the variational formulation

$$\ldots+A_{11}\frac{\partial\delta u}{\partial x}\left[\frac{\partial u}{\partial x}+\frac{1}{2}\left(\frac{\partial w}{\partial x}\right)^2\right]$$
$$+A_{11}\frac{\partial\delta w}{\partial x}\frac{\partial w}{\partial x}\left[\frac{\partial u}{\partial x}+\frac{1}{2}\left(\frac{\partial w}{\partial x}\right)^2\right]+\ldots$$

The first term contributes to the stiffness coefficients K_{ij}^{11} and K_{ij}^{13} (see Appendix), whereas the second term contributes to the stiffness coefficients K_{ij}^{31} and K_{ij}^{33}. Note that

$$K_{ij}^{13}=\int_{\Omega^e}A_{11}\left(\frac{1}{2}\frac{\partial w}{\partial x}\right)\frac{\partial\psi_i}{\partial x}\frac{\partial\psi_j}{\partial x}\mathrm{d}x\mathrm{d}y+\ldots$$
$$K_{ij}^{31}=\int_{\Omega^e}A_{11}\left(\frac{\partial w}{\partial x}\right)\frac{\partial\psi_i}{\partial x}\frac{\partial\psi_j}{\partial x}\mathrm{d}x\mathrm{d}y+\ldots$$

are not the same.

To complete the discretization, we must now approximate the time derivatives appearing in Eq. (13). Here we use the Newmark direct integration method,[24] with $\alpha=0.5$ and $\beta=0.25$ (corresponding to the constant average acceleration method). The scheme, although unconditionally stable for linear problems, is not proven stable for nonlinear problems.

Equation (13) can be expressed, after the application of Newmark's integration scheme, in the form

$$[\hat{K}]\{\Delta\}_{n+1}=\{\hat{F}\}_{n,n+1} \quad (14)$$

where

$$[\hat{K}]=[K]+a_0[M],\ \{\hat{F}\}=\{F\}_{n+1}+[M](a_0\{\Delta\}_n$$
$$+a_1\{\dot{\Delta}\}_n+a_2\{\ddot{\Delta}\}_n),$$
$$a_0=1/(\beta\Delta t^2),\quad a_1=a_0\Delta t,\quad a_2=(1/2\beta)-1 \quad (15)$$

Once the solution $\{\Delta\}$ is known at $t_{n+1}=(n+1)\Delta t$, the first and second derivatives (velocity and accelerations) of $\{\Delta\}$ at t_{n+1} can be computed from

$$\{\ddot{\Delta}\}_{n+1}=a_0(\{\Delta\}_{n+1}-\{\Delta\}_n)-a_1\{\dot{\Delta}\}_n-a_2\{\ddot{\Delta}\}_n$$
$$\{\dot{\Delta}\}_{n+1}=\{\dot{\Delta}\}_n+a_3\{\ddot{\Delta}\}_n+a_4\{\ddot{\Delta}\}_{n+1} \quad (16)$$

where $a_3=(1-\alpha)\Delta t$, and $a_4=\alpha\Delta t$.

All of the operations previously indicated [except for Eq. (16)] can be performed at the element level, and the assembled form of Eq. (14) can be obtained for the whole problem.

$$[K]=[K^L+K^N(\{\Delta\}_{n+1})] \tag{17}$$

where $[K^L]$ denotes the linear stiffness matrix and $[K^N]$ denotes the nonlinear (geometric) stiffness matrix. Because $[K^N]$ depends on the unknown solution $\{\Delta\}_{n+1}$, the assembled equation must be solved iteratively until a convergence criterion is satisfied at time, $t=t_{n+1}$. In the present study the Picard type successive iteration scheme is employed. In this scheme, the nonlinear Eqs. (14) are approximated by the following equation.

$$[\hat{K}(\{\Delta^r\}_{n+1})]\{\Delta^{r+1}\}_{n+1}=\{\hat{F}\}_{n,n+1} \tag{18}$$

where r is the iteration number. In other words, the nonlinear stiffness matrix for the $(r+1)$th iteration is computed using the solution vector from the rth iteration. Such successive iterations are continued until the error

$$E\equiv\left[\sum_{i=1}^{N}|\Delta_i^r-\Delta_i^{r+1}|^2\Big/\sum_{i}^{N}|\Delta_i^r|^2\right] \tag{19}$$

for any fixed time $t=t_{n+1}$, is less than or equal to some preassigned value (say, 1% or less). The iteration at time $t=t_{n+1}$ is stated by using the converged solution at $t=t_n$ (at $t=t_0\equiv 0$, the initial conditions are assumed to be known).

Numerical Results and Discussion

In the present study the nine-node rectangular isoparametric element was employed. The element has either three (w,ψ_x,ψ_y) or five (u,v,w,ψ_x,ψ_y) degrees of freedom (DOF) per node. Because the element accounts for the transverse shear strains, reduced integration was employed to evaluate the shear terms numerically. In other words, the 2×2 Gauss rule was used to integrate the shear energy terms and the 3×3 Gauss rule was used to integrate the bending and inertia terms. All computations were done in double precision on an IBM 3032. In all the numerical examples considered here, zero initial conditions are assumed and damping is neglected.

Because no estimate on the time step for the nonlinear analysis is available in the literature, the critical time step of a conditionally stable finite difference scheme was used as a starting time step, and a convergence study was conducted to select a time step that yielded a stable and accurate solution while keeping the computational time to a minimum. The following two estimates were used in the present study

$$\Delta t_1\leq 0.25(\rho h D)^{1/2}(\Delta x)^2 \tag{20}$$

$$\Delta t_2\leq\left[\rho(1-\nu^2)E\Big/\left\{2+(1-\nu)\frac{\pi^2}{12}\left[1+1.5\left(\frac{\Delta x}{h}\right)^2\right]\right\}\right]^{1/2}\Delta x \tag{21}$$

Here $D=Eh^3/[12(1-\nu^2)]$, and Δx is the minimum distance between the element node points. Estimate Eq. (20), due to Leech,[25] was derived for thin plates, and estimate Eq. (21), due to Tsui and Pin Tong,[26] was derived for thick plates.

First, in order to prove the validity of the present formulation, the results obtained in the present study for isotropic plates are compared with those available in the literature.

1) Simply supported rectangular plate under suddenly applied patch loading (see Fig. 1 and Ref. 27)

$$a=\sqrt{2},\ b=1,\ h=0.1 \text{ and } 0.2,\ \Delta t=0.1,\ q=q_0H(t)$$

$$\begin{aligned} q_0&=10^{-2},\quad 0<x,y\leq 0.2\\ &=0,\qquad x,y>0.2 \end{aligned} \tag{22}$$

$$E_1=E_2=1.0,\ \nu_{12}=0.3,\ \rho=1.0$$

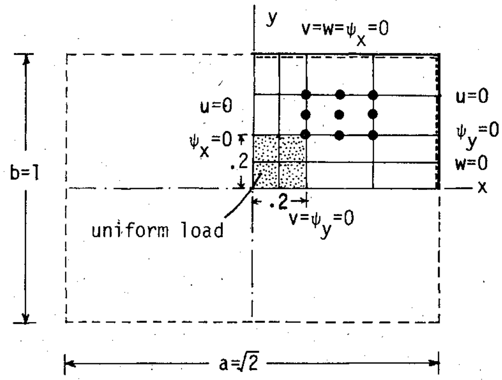

Fig. 1 Finite element mesh and boundary conditions for isotropic rectangular plates under suddenly applied pressure loading at the center.

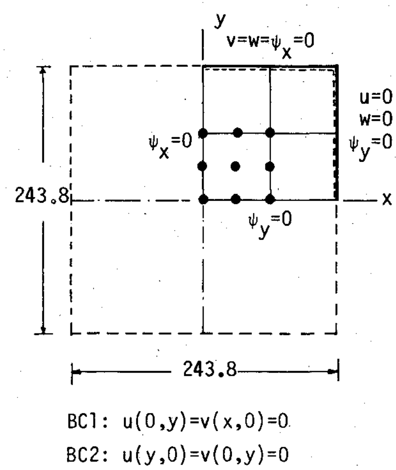

Fig. 2 Finite element mesh and boundary conditions for isotropic square plates under suddenly applied pressure loading.

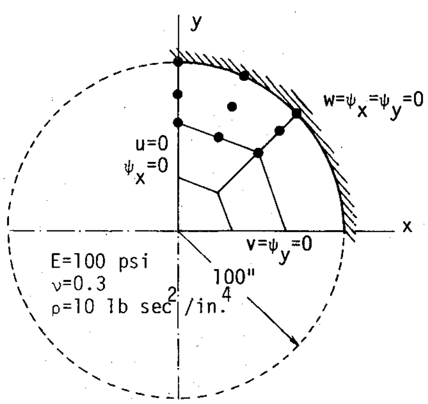

Fig. 3 Finite element mesh and boundary conditions for an isotropic clamped circular plate under suddenly applied pressure loading.

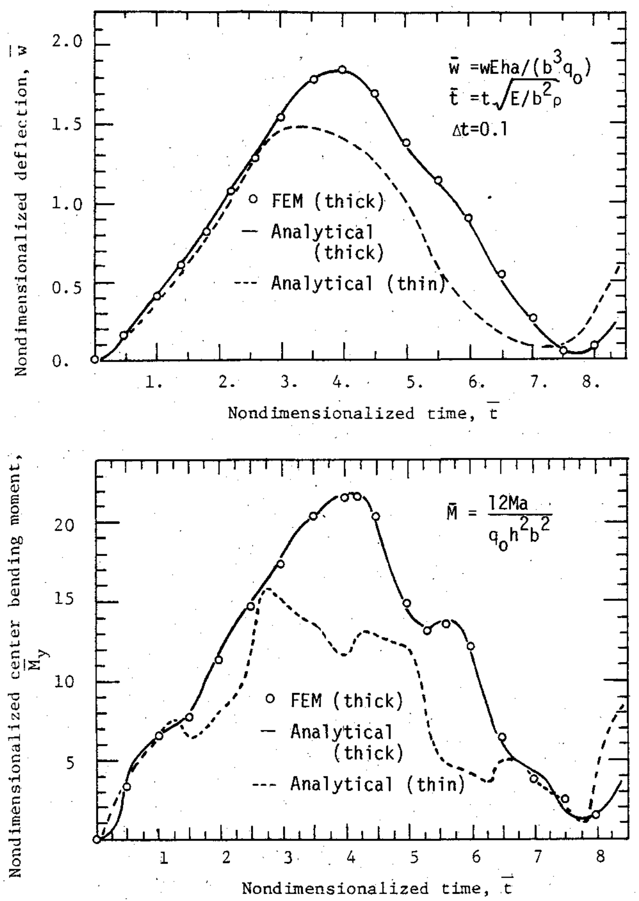

Fig. 4 Nondimensionalized center deflection and bending moment vs nondimensionalized time for simply supported rectangular plates ($\nu = 0.3$) under suddenly applied pressure loading at the center square area (4×4 mesh).

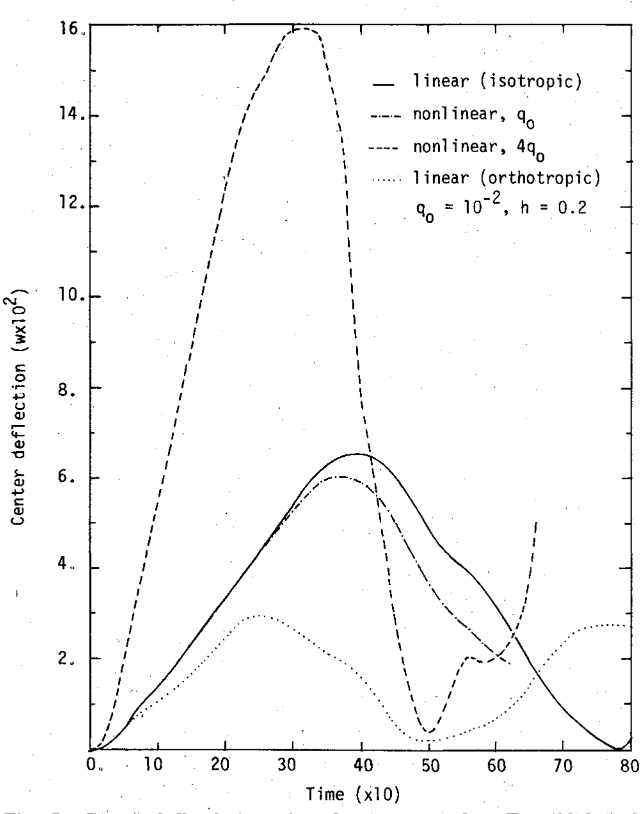

Fig. 5 Center deflection vs time for isotropic [see Eq. (22)] and orthotropic ($E_1 = 25$, $E_2 = 1$, $\nu_{12} = 0.25$, $G_{12} = G_{13} = G_{23} = 0.5E_2$) rectangular plates under suddenly applied loading at the center square area (see Fig. 1).

2) Simply supported square plate under suddenly applied uniformly distributed loading (see Fig. 2 and Ref. 21)

$$a = b = 243.8 \text{ cm}, \; h = 0.635 \text{ cm}, \; \Delta t = 0.005 \text{ s}$$

$$q_0 = 4.882 \times 10^{-4} \text{ N/cm}^2, \; E_1 = E_2 = 7.031 \times 10^5 \text{ N/cm}^2$$

$$\nu_{12} = 0.25, \; \rho = 2.547 \times 10^{-6} \text{ N s}^2/\text{cm}^4 \tag{23}$$

3) Clamped circular plate under suddenly applied uniformly distributed loading (see Fig. 3 and Ref. 19).

$$R\,(\text{radius}) = 100 \text{ cm}, \; h = 10 \text{ and } 20 \text{ cm}, \; \Delta t = 2.5 \text{ s}$$

$$q_0 = 1.0 \text{ N/cm}^2, \; E_1 = E_2 = 100 \text{ N/cm}^2, \; \nu_{12} = 0.3$$

$$\rho = 10 \text{ Ns}^2/\text{cm}^4 \tag{24}$$

A. Simply Supported, Rectangular, Isotropic and Orthotropic Plates

A 4×4 (nonuniform) mesh is used in the quarter plate with three degrees of freedom per node. The center deflection and bending moments of the present linear analysis are compared with the analytical thick-plate and thin-plate solutions of Reismann and Lee[27] in Fig. 4. We note pronounced difference between the solutions of the two theories. The deviation between the solutions of the shear deformation theory and the classical theory increases with plate thickness. The present finite element solutions for the center deflection and bending moment are in excellent agreement with those of Reismann and Lee.[27]

The center deflections obtained in the present linear and nonlinear analysis are presented in Fig. 5. To show the effect of material orthotropy on the center deflection, results of the linear analysis of an orthotropic plate ($E_1/E_2 = 25$, $\nu_{12} = 0.25$) are also included in Fig. 5. The effect of orthotropy and geometric nonlinearity on the amplitude and period of nondimensionalized center deflection of orthotropic plates ($E_1/E_2 = 25$, $\nu_{12} = 0.25$) is apparent from the plots presented in Fig. 5; the effect of orthotropy is to decrease both amplitude and period of the center deflection, and the effect of the nonlinearity is to decrease the amplitude, and smoothen the solution somewhat. The effect of the plate thickness on the amplitude and period of the nondimensionalized center deflection (linear) $\bar{w} = 10wE_2h^3/q_0a^4$, can be seen from the plots in Fig. 6. The amplitude decreased about 30% for a decrease in thickness from $b/h = 0.2$ to $b/h = 0.1$.

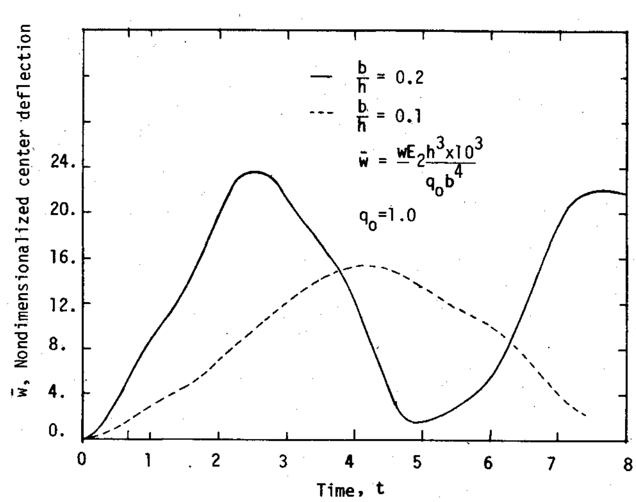

Fig. 6 Effect of plate thickness on the transient response of orthotropic plates (see Fig. 5 for material properties) under suddenly applied patch loading (i.e., load on the square area at the center of the rectangular plate).

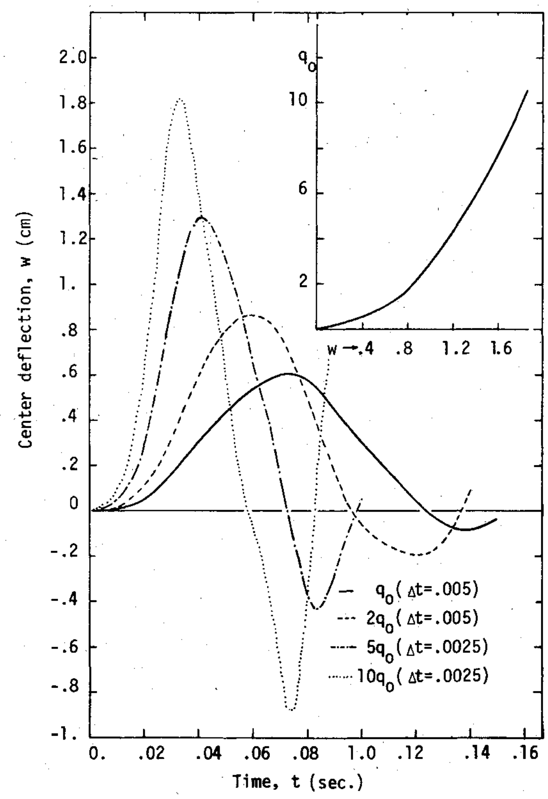

Fig. 7 Nonlinear transient response of isotropic plates [see Eq. (23) and Fig. 2 for the data and finite element mesh and boundary conditions] under suddenly applied uniformly distributed loads.

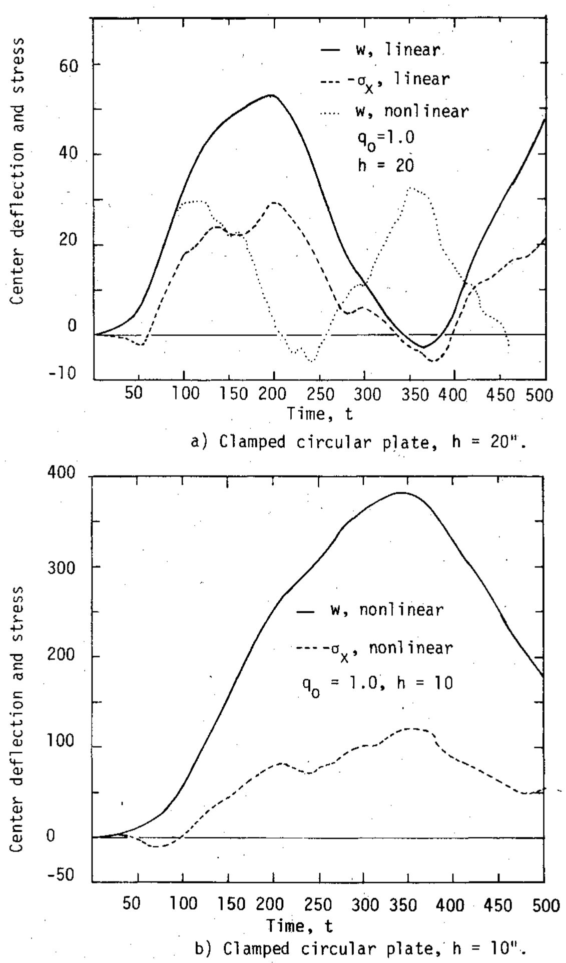

Fig. 8 Transient response of a clamped, isotropic, circular plate under suddenly applied transverse load (see Fig. 3 for the finite element mesh and boundary conditions).

B. Simply Supported Square Plates (BC1)

A 2×2 (uniform) mesh is used in the quarter plate with five degrees of freedom per node. Results of the present nonlinear analysis (see Fig. 7) agree closely with the mixed finite element results of Akay.[21] The plots of center deflection vs time for various loads are shown in Fig. 7 along with the load-deflection curve. Note that amplitude and period of the center deflection decrease with increasing values of the load. Further note that the negative peak also increases with decreasing load.

C. Clamped Circular Plates

Results of the linear transient analysis of the clamped square plate, for two different thicknesses, are presented in Figs. 8a and 8b. The present results agree with those reported by Hinton.[19] The effect of the decrease in thickness is to increase the amplitude and period of the center deflection and stress. Figure 8a also contains plots of center deflection of the linear and nonlinear analysis. The effect of the (von Kármán type) nonlinearity is to decrease the amplitude and period of the center deflection and stress.

The results of the nonlinear analysis of layered composite plates are presented next. Due to the bending-stretching coupling in composite plates, we cannot assume the biaxial symmetry even when the plate is geometrically symmetric and load is symmetric. To show the effect, the full plate model (4×4 mesh of nine-node elements) and quarter plate model (2×2 mesh of nine-node elements) were used to analyze a

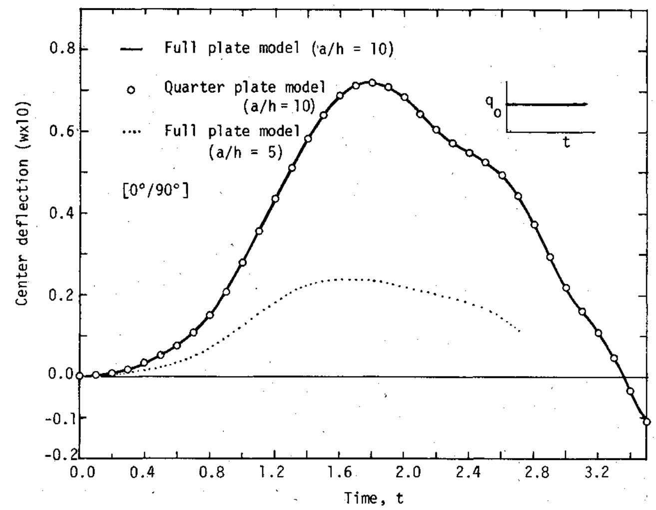

Fig. 9 The effect of plate thickness and finite element models used to analyze the transient response on the center deflection of the plate.

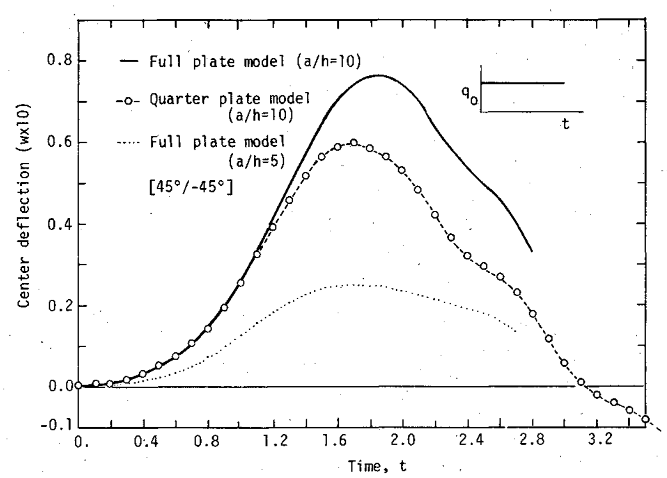

Fig. 10 The effect of plate thickness and finite element models used to analyze the transient response on the center deflection.

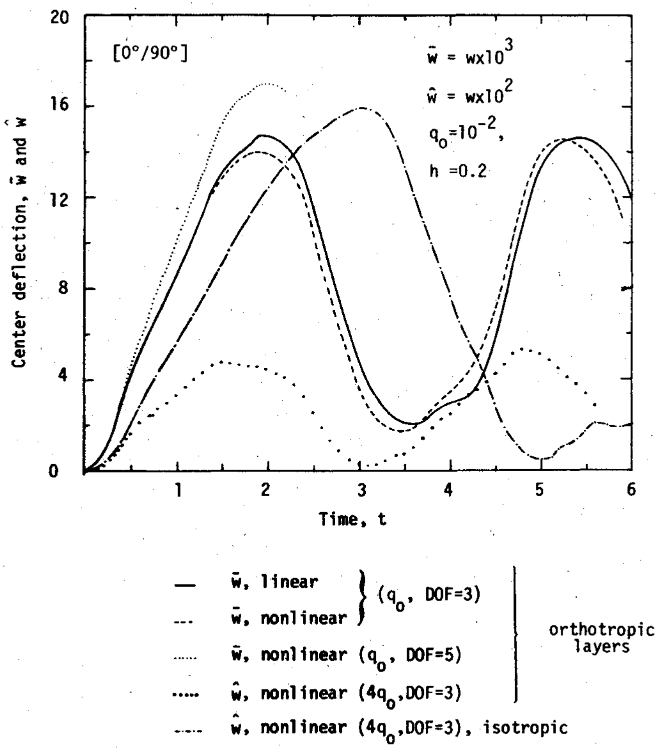

Fig. 11 Transient response of two-layer cross-ply [0°/90°] rectangular plates under suddenly applied patch loading [see Eq. (22) and Fig. 1 for the data and mesh information; see Eq. (25) for the material properties].

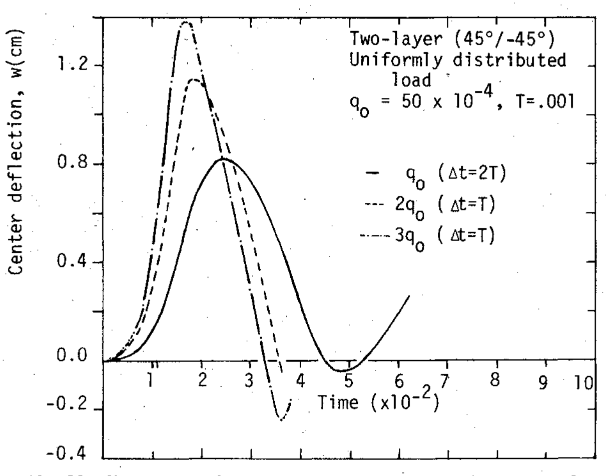

Fig. 12 Nonlinear transient response of laminated square plates under suddenly applied uniform loading [see Eq. (25) for the material properties].

simply supported (BC1) square plate ($a/b=1$, $a/h=10$) under uniform load ($q_0=0.005$). The material properties are assumed to be

$$E_1/E_2=25,\ G_{12}=G_{13}=0.5E_2,\ G_{23}=0.2E_2,\ \nu_{12}=0.25 \tag{25}$$

A time step of 0.1 was used in the analysis. Figure 9 contains the plot of the center deflection vs time for two-layer, [0°/90°], cross-ply plate. For the particular choice of the symmetry boundary conditions (BC1), the full plate model and the quarter plate models yield virtually the same results. This is expected because the mode shapes for the displacement field (see Reddy[16]) satisfy the symmetry boundary condition in BC1. To further investigate the effect of the coupling on the plate response, a two-layer angle-ply

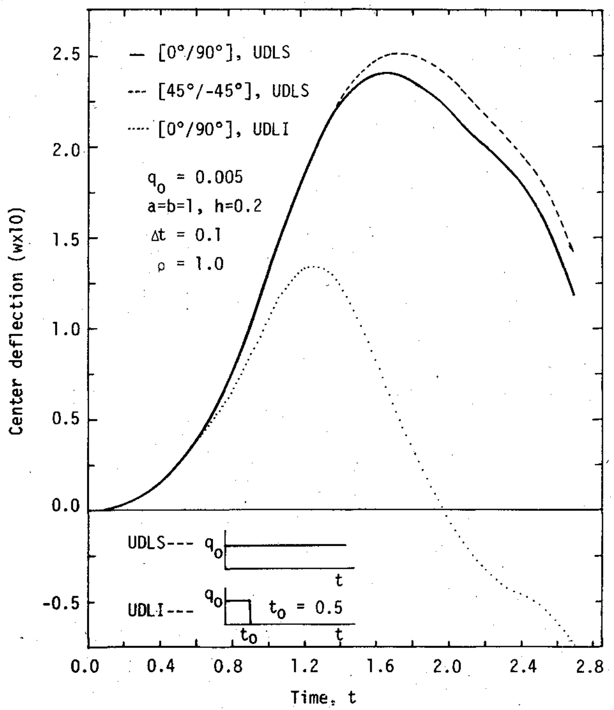

Fig. 13 The effect of the lamination scheme and loading on the center deflection of simply supported square plates [see Eq. (25) for the material properties, and Figs. 9 and 10 for other information].

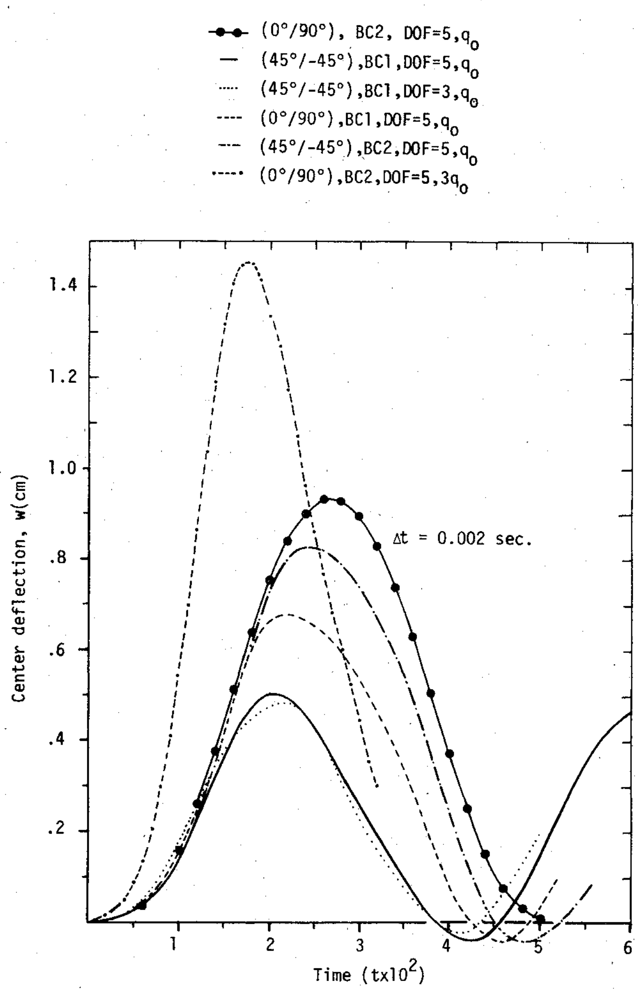

Fig. 14 Effect of the boundary conditions (BC1 and BC2) on the nonlinear transient response of laminated square plates under suddenly applied transverse, uniformly distributed, loading [see Eq. (23) for the data and Fig. 2 for the mesh and boundary conditions; orthotropic properties of layers are given in Eq. (25)].

[45°/−45°], square plate was analyzed using the same symmetry boundary conditions (BC1). From Fig. 10 it is clear that the responses predicted by the full plate model and the quarter plate model differ from each other. This can be explained again in terms of the mode shapes for the angle-ply plate (see Ref. 16), which do not satisfy the symmetry boundary conditions in BC1 but satisfy the symmetry boundary conditions in BC2 (see Fig. 2). Similar observations can be made by interchanging the symmetry boundary conditions BC1 and BC2 for the cross-ply and angle-ply plates. Figures 9 and 10 also contain plots of the center deflection vs time for plate side-to-thickness ratio of 5. The effect of the thickness on the amplitude of the deflection is apparent from the plots.

The results discussed in the following paragraphs were obtained using the quarter plate models. For the cross-ply plates the symmetry boundary conditions of BC1 were used, and for the angle-ply plates the symmetry conditions of BC2 were used. The effect of the symmetry boundary conditions on the transient response obtained using the quarter plate model is also discussed later in this section.

Figure 11 contains the plot of the center deflection vs time for a simply supported (BC1) two-layer cross-ply, [0°/90°], plate. The same data (except for the material properties) as in Eq. (22) are used. The effect of coupling between the inplane displacements and bending deflections is to increase the amplitude of the center deflection.

The plot of the center deflection vs time for a two-layer, angle-ply [45°/−45°], plate under suddenly applied uniform loading is presented in Fig. 12. The data used are the same as that in Eq. (23), except for the material properties. The effect of the nonlinearity on the amplitude and period of the center deflection is apparent from the results presented in Fig. 12. Note that the rate of increase in the amplitude of the center deflection decreases with increasing load.

Figure 13 contains plots of the center deflection vs time for two-layer cross-ply [0°/90°] and angle-ply [45°/−45°] plates under uniformly distributed step loading. The plots are included to show the difference between the response of a cross-ply plate and angle-ply plate. The figure also contains results for the cross-ply plate for the case when the load is removed at time $t=0.5$.

Finally, the effect of boundary conditions (BC1 and BC2) on the center deflection of two-layer square plates under uniformly distributed load was investigated; Fig. 14 contains results of the investigation. It is clear that the response of cross-ply as well as angle-ply plates under BC1 differ significantly from the results of plates under BC2. Note also that suppression of the inplane degrees of freedom results in about 50% decrease in the center deflection of angle-ply [45°/−45°] plates.

Summary and Conclusions

A shear flexible finite element that accounts for the von Kármán strains is employed in the transient analysis of layered composite plates. The present results for isotropic plates are very close to the analytical and other finite element solutions available in the literature. The present results of layered composite plates should serve as reference solutions for future investigations. Although the paper contains results for certain geometries, loadings, lamination scheme, and material properties, it should be pointed out that the element developed herein can be employed to laminated plates of arbitrary geometry, lamination scheme, material properties, boundary conditions, and loading (the only limitations are those inherent in the laminated plate theory used). The present analysis does not account for material damping effects; studies of composite plates accounting for material damping and material nonlinearities are awaiting attention.

Appendix: Elements of Stiffness and Mass Matrices

Stiffness matrix

$$[K]=\begin{bmatrix} [K^{11}] & [K^{12}] & [K^{13}] & [K^{14}] & [K^{15}] \\ [K^{21}] & [K^{22}] & [K^{23}] & [K^{24}] & [K^{25}] \\ [K^{31}] & [K^{32}] & [K_1^{33}]+[K_2^{33}] & [K_1^{34}]+[K_2^{34}] & [K_1^{35}]+[K_2^{35}] \\ [K^{41}] & [K^{42}] & [K_1^{43}]+[K_2^{43}] & [K^{44}] & [K^{45}] \\ [K^{51}] & [K^{52}] & [K_1^{53}]+[K_2^{53}] & [K^{54}] & [K^{55}] \end{bmatrix}$$

Mass matrix

$$[M]=\begin{bmatrix} P[S] & [0] & [0] & R[S] & [0] \\ [0] & P[S] & [0] & [0] & R[S] \\ [0] & [0] & P[S] & [0] & [0] \\ R[S] & [0] & [0] & I[S] & [0] \\ [0] & R[S] & [0] & [0] & I[S] \end{bmatrix}$$

The matrix coefficients $K_{ij}^{\alpha\beta}$ are given by

$$[K^{11}]=A_{11}[S^{xx}]+A_{16}([S^{xy}]+[S^{xy}]^T)+A_{66}[S^{yy}]$$

$$[K^{12}]=A_{12}[S^{xy}]+A_{16}[S^{xx}]+A_{26}[S^{yy}]+A_{66}[S^{xy}]^T=[K^{21}]^T$$

$$[K^{13}]=A_{11}[R_x^{xx}]+A_{12}[R_y^{xy}]+A_{16}([R_x^{xy}]+[R_x^{xy}]^T$$
$$+R_y^{xx}])+A_{26}[R_y^{yy}]+A_{66}([R_y^{xy}]^T+[R_x^{yy}])=\tfrac{1}{2}[K^{31}]^T$$

$$[K^{14}]=B_{11}[S^{xx}]+B_{16}([S^{xy}]+[S^{xy}]^T)+B_{66}[S^{yy}]=[K^{41}]^T$$

$$[K^{15}]=B_{12}[S^{xy}]+B_{16}[S^{xx}]+B_{26}[S^{yy}]+B_{66}[S^{xy}]^T=[K^{51}]^T$$

$$[K^{22}]=A_{22}[S^{yy}]+A_{26}([S^{xy}]^T+S^{xy}])+A_{66}[S^{xx}]$$

$$[K^{23}]=A_{12}[R_x^{xy}]^T+A_{22}[R_y^{yy}]+A_{26}([R_y^{xy}]^T+[R_y^{xy}]+[R_x^{yy}])$$
$$+A_{16}[R_x^{xx}]+A_{66}([R_x^{xy}]^T+[R_y^{xx}])=\tfrac{1}{2}[K^{32}]^T$$

$$[K^{24}]=B_{12}[S^{xy}]^T+B_{26}[S^{yy}]+B_{16}[S^{xx}]+B_{66}[S^{xy}]=[K^{42}]^T$$

$$[K^{25}]=B_{22}[S^{yy}]+B_{26}([S^{xy}]+[S^{xy}]^T)+B_{66}[S^{xx}]=[K^{52}]^T$$

$$[K_1^{33}]=A_{55}[S^{xx}]+A_{45}([S^{xy}]+[S^{xy}]^T)+A_{44}[S^{yy}]$$

$$[K_2^{33}]=\frac{1}{2}\int_{\Omega^e}\left[\bar{N}_1\frac{\partial\phi_i}{\partial x}\frac{\partial\phi_j}{\partial x}+\bar{N}_6\left(\frac{\partial\phi_i}{\partial x}\frac{\partial\phi_j}{\partial y}+\frac{\partial\phi_i}{\partial y}\frac{\partial\phi_j}{\partial x}\right)\right.$$
$$\left.+\bar{N}_2\frac{\partial\phi_i}{\partial y}\frac{\partial\phi_j}{\partial y}\right]\mathrm{d}x\mathrm{d}y$$

$$[K_1^{34}]=A_{55}[S^{x0}]+A_{45}[S^{y0}]=[K_1^{43}]^T$$

$$[K_2^{34}]=B_{11}[R_x^{xx}]+B_{16}([R_x^{xy}]+[R_x^{xy}]^T+[R_y^{xx}])+B_{12}[R_y^{xy}]^T$$
$$+B_{26}[R_y^{yy}]+B_{66}([R_x^{yy}]+[R_y^{xy}])=2[K_2^{43}]^T$$

$$[K_1^{35}]=A_{45}[S^{x0}]+A_{44}[S^{y0}]=[K_1^{53}]^T$$

$$[K_2^{35}]=B_{12}[R_x^{xy}]+B_{16}[R_x^{xx}]+B_{22}[R_y^{yy}]+B_{26}([R_y^{xy}]^T$$
$$+[R_x^{yy}]+[R_y^{xy}])+B_{66}([R_x^{xy}]^T+[R_y^{xx}])=2[K^{53}]^T$$

$$[K^{44}] = D_{11}[S^{xx}] + D_{16}([S^{xy}] + [S^{xy}]^T) + D_{66}[S^{yy}] + A_{55}[S]$$

$$[K^{45}] = D_{12}[S^{xy}] + D_{16}[S^{xx}] + D_{26}[S^{yy}]$$

$$+ D_{66}[S^{xy}]^T + A_{45}[S] = [K^{54}]^T$$

$$[K^{55}] = D_{26}([S^{xy}] + [S^{xy}]^T) + D_{66}[S^{xx}] + D_{22}[S^{yy}] + A_{44}[S]$$

and

$$S_{ij}^{\xi\eta} = \int_{\Omega^e} \frac{\partial\phi_i}{\partial\xi}\frac{\partial\phi_j}{\partial\eta}\mathrm{d}x\mathrm{d}y, \quad \xi,\eta = 0,x,y$$

$$S_{ij}^{00} \equiv \int_{\Omega^e} \phi_i\phi_j \mathrm{d}x\mathrm{d}y$$

$$R_{\zeta}^{\xi,\eta} = \int_{\Omega^e} \frac{1}{2}\left(\frac{\partial w}{\partial\zeta}\right)\frac{\partial\phi_i}{\partial\xi}\frac{\partial\phi_j}{\partial\eta}\mathrm{d}x\mathrm{d}y, \quad \zeta,\xi,\eta = 0,x,y$$

$$\bar{N}_1 = A_{11}\left(\frac{\partial w}{\partial x}\right)^2 + A_{12}\left(\frac{\partial w}{\partial y}\right)^2 + 2A_{16}\frac{\partial w}{\partial x}\frac{\partial w}{\partial y}$$

$$\bar{N}_2 = A_{12}\left(\frac{\partial w}{\partial x}\right)^2 + A_{22}\left(\frac{\partial w}{\partial y}\right)^2 + 2A_{26}\frac{\partial w}{\partial x}\frac{\partial w}{\partial y}$$

$$\bar{N}_6 = A_{16}\left(\frac{\partial w}{\partial x}\right)^2 + A_{26}\left(\frac{\partial w}{\partial y}\right)^2 + 2A_{66}\frac{\partial w}{\partial x}\frac{\partial w}{\partial y}$$

Acknowledgments

The results reported in this paper were obtained during an investigation supported by the Structural Mechanics Program of the Air Force Office of Scientific Research (Grant AFOSR-81-0142). The author is grateful to Dr. Anthony Amos (AFOSR) for his encouragement and support of this work. Sincere thanks are also due to Professor R. M. Jones for his comments, which led to an improved manuscript.

References

[1] Lamb, H., "On Waves in an Elastic Plate," *Proceedings of the Royal Society of London*, Series A, Vol. 93, 1917, p. 114.

[2] David, N. and Lawhead, W., "Transient Analysis of Oblique Impact on Plates," *Journal of the Mechanics and Physics of Solids*, Vol. 13, 1965, p. 199.

[3] Timoshenko, S., "On the Correction for Shear of the Differential Equation for Transverse Vibrations of Prismatic Bars," *Philosophical Magazine*, Ser. 6, Vol. 41, 1921, p. 744.

[4] Reissner, E., "The Effects of Transverse Shear Deformation on the Bending of Elastic Plates," *Journal of Applied Mechanics, Transactions of ASME*, Vol. 67, 1945, p. A-69.

[5] Reissner, E., "On Bending of Elastic Plates," *Quarterly of Applied Mathematics*, Vol. 5, 1947, p. 55.

[6] Mindlin, R. D., "Influence of Rotatory Inertia and Shear on Flexural Motions of Isotropic, Elastic Plates," *Journal of Applied Mechanics*, Vol. 18, 1951, p. 31.

[7] Yang, P. C., Norris, C. H., and Stavsky, Y., "Elastic Wave Propagation in Heterogeneous Plates," *International Journal of Solids and Structures*, Vol. 2, 1966, pp. 665-684.

[8] Medwadowski, S. J., "A Refined Theory of Elastic, Orthotropic Plates," *Journal of Applied Mechanics*, Vol. 25, 1958, pp. 437-443.

[9] Ebcioglu, I. K., "A Large Deflection Theory of Anisotropic Plates," *Ingenieur-Archiv*, Vol. 33, 1964, pp. 396-403.

[10] Moon, F. C., "Wave Surfaces Due to Impact on Anisotropic Plates," *Journal of Composite Materials*, Vol. 6, 1972, pp. 62-79.

[11] Moon, F. C., "One-Dimensional Transient Waves in Anisotropic Plates," *Journal of Applied Mechanics*, Vol. 40, 1973, pp. 485-490.

[12] Chow, T. S., "In the Propagation of Flexural Waves in an Orthotropic Laminated Plate and its Response to an Impulsive Load," *Journal of Composite Material*, Vol. 5, 1971, pp. 306-319.

[13] Wang, A.S.D., Chou, P. C., and Rose, J. L., "Strongly Coupled Stress Waves in Heterogeneous Plates," *AIAA Journal*, Vol. 10, 1972, pp. 1088-1090.

[14] Sun, C. T. and Whitney, J. M., "Dynamic Response of Laminated Composite Plates," *AIAA Journal*, Vol. 13, Oct. 1975, pp. 1250-9-1260.

[15] Whitney, J. M. and Sun, C. T., "Transient Response of Laminated Composite Plates Subjected to Transverse Dynamic Loading," *Journal of the Acoustics Society of America*, Vol. 61, No. 1, 1977, pp. 101-104.

[16] Reddy, J. N., "On the Solutions to Forced Motions of Layered Composite Plates," *Journal of Applied Mechanics*, Vol. 104, 1982, pp. 403-408.

[17] Reddy, J. N., "Dynamic (Transient) Analysis of Layered Anisotropic Composite-Material Plates," *International Journal of Numerical Methods in Engineering*, to appear.

[18] Hinton, E., Owen, D.R.J., and Shantaram, D., "Dynamic Transient Linear and Nonlinear Behavior of Thick and Thin Plates," *The Mathematics of Finite Elements and Applications II*, edited by J. R. Whiteman, Academic Press, London, 1976.

[19] Hinton, E., "The Dynamic Transient Analysis of Axisymmetric Circular Plates by the Finite Element Method," *Journal of Sound and Vibration*, Vol. 46, 1976, pp. 465-472.

[20] Pica, A. and Hinton, E., "Transient and Pseudo-Transient Analysis of Mindlin Plates," *International Journal of Numerical Methods in Engineering*, Vol. 15, 1980, pp. 189-208.

[21] Akay, H. U., "Dynamic Large Deflection Analysis of Plates Using Mixed Finite Elements," *Computers and Structures*, Vol. 11, 1980, pp. 1-11.

[22] Jones, R. M., *Mechanics of Composite Materials*, McGraw-Hill, New York, 1975.

[23] Reddy, J. N., "A Penalty Plate-Bending Element for the Analysis of Laminated Anisotropic Composite Plates," *International Journal of Numerical Methods in Engineering*, Vol. 15, 1980, pp. 1187-1206.

[24] Bathe, K. J. and Wilson, E. L., *Numerical Methods in Finite Element Analysis*, Prentice-Hall, Englewood Cliffs, N.J., 1976.

[25] Leech, J. W., "Stability of Finite Difference Equations for the Transient Response of a Flat Plate," *AIAA Journal*, Vol. 3, Sept. 1965, pp. 1772-1773.

[26] Tsui, T. Y. and Tong, P., "Stability of Transient Solution of Moderately Thick Plate by Finite Difference Method," *AIAA Journal*, Vol. 9, 1971, pp. 2062-2063.

[27] Reismann, H. and Lee, Y., "Forced Motions of Rectangular Plates," *Developments in Theoretical and Applied Mechanics*, Vol. 4, edited by D. Frederick, Pergamon Press, New York, 1969, pp. 3-18.